10th INTERNATIONAL SCIENTIFIC CONFERENCE
ON DEFENSIVE TECHNOLOGIES
OTEH 2022
Belgrade, Serbia, 13 – 14 October 2022

NUMERICAL ANALYSIS OF THE INHOMOGENEOUS OBSTACLE INFLUENCE ON THE PRECURSOR SHAPED CHARGE WARHEAD PERFORMANCE

MILOŠ MARKOVIĆ
University of Belgrade, Faculty of Mechanical Engineering, Belgrade, mdmarkovic@mas.bg.ac.rs

PREDRAG ELEK
University of Belgrade, Faculty of Mechanical Engineering, Belgrade, pelek@mas.bg.ac.rs

DEJAN JEVTIĆ
University of Belgrade, Faculty of Mechanical Engineering, Belgrade, djevtic@mas.bg.ac.rs

RADOVAN ĐUROVIĆ
University of Belgrade, Faculty of Mechanical Engineering, Belgrade, rdjurovic@mas.bg.ac.rs

IVANA TODIĆ
University of Belgrade, Faculty of Mechanical Engineering, Belgrade, itodic@mas.bg.ac.rs

Abstract: *Purpose of the precursor shaped charge warhead is to initiate the Explosive Reactive Armor (ERA) and thus provide an unobstructed path to the jet of the main shaped charge. The precursor warhead is most commonly placed in the front of the missile where it is surrounded by other subsystems. All of the subsystems which lay on the path of the precursor warhead's shaped charge jet represent the obstacle that will decrease its efficiency. The goal of this paper is to analyze the precursor warhead's performance in a case where the inhomogeneous obstacle is placed in front of it. The numerical analysis of the obstructed formation process was performed in order to determine the properties of the formed jet using ANSYS AUTODYN 2D software. For the existing missile configuration, jet formation process and precursor warhead's performance against ERA were analyzed numerically. Significant differences in formed jet's properties were observed for the simulations with and without the inhomogeneous obstacles. In the case of inhomogeneous obstacle it is present decreasing of jet tip velocity for around 23%, decreasing of jet tip dimaeter for around 50% and jet time are delayed in contact with ERA front panel for around 10 μs. Obtained results indicate that in the observed cases, formed jet has enough energy to initiate the explosive reactive armor.*

Keywords: *numerical analysis, shaped charge, precursor warhead, explosive reactive armor.*

1. INTRODUCTION

In the early stages of missile design, it is highly important to determine payload subsystem's configuration and position. Antitank missile's design and its subsystems placement strongly depend on its tactical-technical requirements. In a case of a missile that contains a homing head, it will inevitably be placed in its front section where it will be surrounded with various electronic components, optical lenses, power supply etc. Majority of those parts will be placed in front of a precursor shaped charge warhead leading to the occurrence of their interaction during the jet formation process that will decrease jet's performance against the ERA. Due to that, it is highly important to clarify whether or not a precursor shaped charge will be able to penetrate all of the aforementioned obstacles and activate explosive reactive armor.

ANSYS AUTODYN software is widely used in the fields of warhead design [1], physics of explosion [1,2], terminal ballistics etc. as it is able to successfully simulate blast, fragmentation and penetration processes [3-8]. Yanan et al. [9] have investigated penetration performance of the main shaped charge warhead in presence of other missile subsystems placed in front of it. Missile configuration in that research doesn't include precursor shaped charge warhead. Numerical model was developed in order to test different stand-offs for optimal solution determination. Chang et al. [10] have analyzed low-density jet penetration into the explosive reactive armor by the means of numerical simulation. For the ERA's explosive, COMP B with the Lee-Tarver's equation of state was selected as it is able to simulate the process of ignition and growth. Results indicate that the observed low-density jet has sufficient energy and is able to activate the explosive reactive armor. Liangliang et al. [11] numerically simulated jet formability and damage characteristics for the low-density liner material. Furthermore, theoretical and empirical initiation criteria of ERA was presented and the analysis of ERA's reaction degree coefficient was displayed. In the present research, numerical investigation was performed in ANSYS

AUTODYN software in order to determine to which degree the inhomogeneous obstacles in front of precursor warhead deteriorate its properties for the real missile configuration. All of the observed processes, including the detonation wave propagation, jet formation, penetration through the inhomogeneous obstacles and the interaction with ERA were simulated using the Euler 2D Multi-material solver. Shaped charge jet's properties were tracked using the fix gauge points placed along the symmetry axis. In addition, a simulation was performed without the obstacles to serve as a reference.

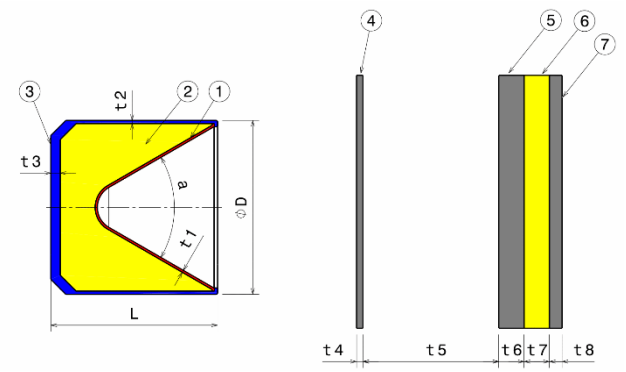

a) b)

Figure 1. Configuration of the analyzed precursor shaped charge and ERA with main dimensions

2. NUMERICAL ANALYSIS

2.1. Warhead and ERA configuration

Investigated precursor shaped charge warhead may be seen in Fig.1(a). It consists of a copper liner (pos.1), high explosive charge (pos. 2) and aluminum casing (pos.3).

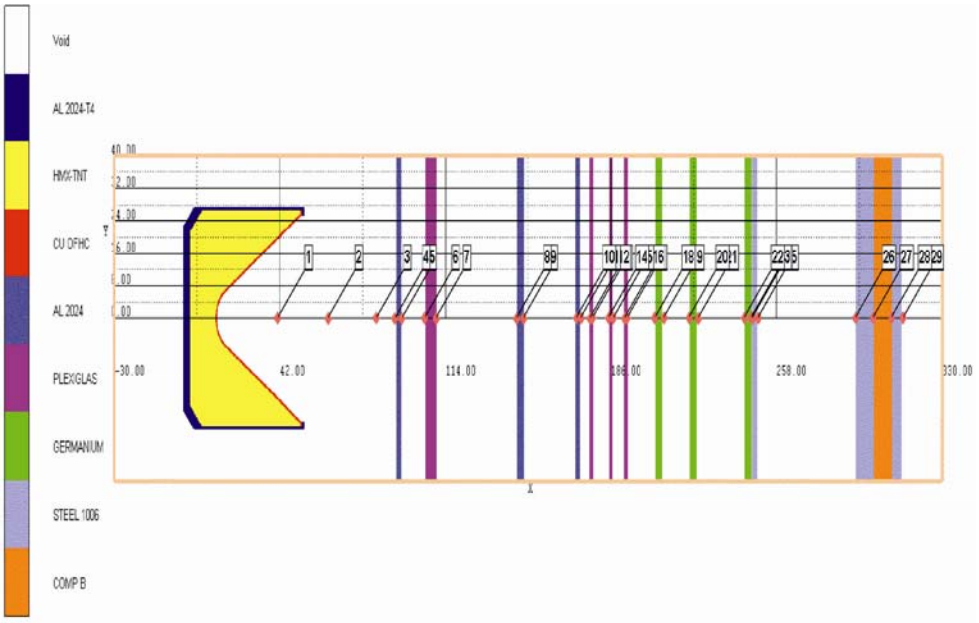

Figure 2. Geometry of the developed numerical model and the Euler domain

First generation of explosive reactive armor is investigated due to its extensive usage for the vehicle protection. As described in ref. [12], it comprises a steel container box (pos. 4) followed by a sandwich made from front steel panel (pos. 5), explosive charge (pos. 6) and rear steel panel (pos. 7) (Fig.1(b)). Dimensions of both the precursor shaped charge and the explosive reactive armor may be found in Table 1. Stand-off distance from the ERA's front metal plate was kept constant in both of the analyzed cases with its value being equal to 3.5 calibers.

Table 1. Shaped charge and ERA dimensions

Precursor shaped charge	
Length	L = 53 mm
Diameter	D = 55 mm
Liner thickness	t1 = 0.75 mm
Confinement thickness side	t2 = 1.5 mm
Confinement thickness bottom	t3 = 3 mm
Liner angle	a = 55º
Explosive reactive armor	
Container thickness	t4 = 2 mm
Distance	t5 = 45mm
Front panel thickness	t6 = 8 mm
Explosive charge thickness	t7 = 8 mm
Rear panel thickness	t8 = 4 mm

2.2. Numerical model setup

Two-dimensional axisymmetric numerical model was developed using the Euler, 2D Multi-material solver. In Fig.2, Finite Element model of the precursor shaped charge, inhomogeneous obstacles and the ERA is displayed. The model is mirrored about the symmetry axis for the better visualization. Dimensions of the rectangular domain are 360x40 mm and their selection was based on the two geometrical conditions. The first one is related to length of the missile's front section and the length of the ERA while the second one is related to the precursor

shaped charge warhead's diameter. In order to avoid occurrence of the wave refraction, "flow out" boundary condition was set on the domain's outer edges. Grade zoning was applied in the lower J-direction with fixed cell size of dy=0.1mm and the nJ=30 times. There are several reasons for the implementation of the grade zoning: diameter of the formed jet is relatively small when compared to the diameter of the obstacles and ERA, jet formation and penetration processes are concentrated in the vicinity of the symmetry axis and it provides better mesh quality while keeping the number of elements unchanged. In the axial direction of the rectangular domain, constant element size of 0.2 mm was chosen. In total, 360000 mesh elements were created. Furthermore, 29 fixed gauge points were placed along the axis of symmetry in order to detect the changes in jet's properties during its formation and throughout the process of interaction with the obstacles.

2.3. Material models

Liner of the investigated shaped charge was made from copper. Zerilli-Armstrong strength model was selected for its behavior modeling as it is advantageous when compared to the other strength models available in hydro-code numerical simulations [13]. Parameters for the equation of state and strength model were adopted from the AUTODYN material library and are given in Table 2.

Table 2. Material properties of OFHC cooper

Reference Density	8.96g/cm3
EOS	Linear
Bulk Modulus	1.29e+08 kPa
Ref. Temperature	295.149994 K
Specific Heat	383 J/kgK
Strength Model	Zerilli Armstrong
Shear Modulus	4.6e+07 kPa
Yield Stress	6.5e+04 kPa
Hardening Constant #2	8.9e+05 kPa
Hardening Constant #4	115e-04 (none)
Ref. Strain Rate (/s)	1

Explosives used in the simulations are HMX-TNT for the shaped charge and COMP B for the ERA. Both of them are available in the AUTODYN's standard material library with the Jones-Wilkins-Lee (JWL) equation of state for which the parameters are given in Table 3. Initiation of the ERA's explosive due to the impact of the shaped charge's jet may be modeled using the complex Lee-Tarver model which describes initiation and growth of the detonation due to the occurrence of shock pressure. Nevertheless, similar results may be obtained by adding two more parameters to the JWL equation. Those parameters are known as burn on compression fraction and pre-burn bulk modulus for which the values can be found in available experimental reports for commonly used explosives.

Table 3. Properties of the implemented explosives

HMX-TNT	
Reference Density	1.776 g/cm3
EOS	JWL
Parameter A	7.0079E+08 kPa
Parameter B	1.2116e+07 kPa
Parameter R1	4.5
Parameter R2	1.1
Parameter W	0.3
C-J Detonation velocity	8.21e+03 m/s
C-J Energy/unit volume	8.899536e+06 kJ/m3
C-J Pressure	3.11e+07 kPa
COMP B	
Reference Density	1.776 g/cm3
EOS	JWL
Parameter A	5.2423e+08 kPa
Parameter B	7.678e+06 kPa
Parameter R1	4.2
Parameter R2	1.1
Parameter W	0.34
C-J Detonation velocity	7.98e+03 m/s
C-J Energy/unit volume	8.585e+06 kJ/m3
C-J Pressure	2.95e+07 kPa
Burn on compression frac.	0.8
Pre-burn bulk modulus	4.343697e+06 kPa

Equations of state and strength models for the materials of the obstacles which are located in front of the precursor shaped charge are given in Table 4, while their purpose, thickness and axial positions are enlisted in Table 5. Position of each obstacle was measured from the reference coordinate system placed on the rear edge of the precursor shaped charge warhead up to the component's closest edge.

Table 4. EOS and strength models of the inhomogeneous obstacle materials

Material name	Equation of state	Strength model	Failure model
AL2024-T4	Shock	Steinberg Guinan	None
HMX-TNT	JWL	None	None
CU OFHC	Linear	Zerili Armstrong	None
AL 2024	Shock	None	None
PLEXIGLAS	Shock	None	None
GERMANIUM	Shock	None	None
STEEL 1006	Shock	Johnson Cook	None
COMP B	JWL	None	None

Inhomogeneous obstacles comprise elements of the missile's autopilot (pos.1–3), TV homing head's electromechanical components (pos.4–7), and TV homing head's optics (pos. 8–10).

Table 5. Properties of the inhomogeneous obstacles

Pos.	Purpose	Material	Thickness [mm]	Position [mm]
1	Carrier	AL2024	2	93
2	PCB	PVC	5	105
3	Carrier	AL2024	3	145
4	Carrier	AL2024	2	170
5	PCB	PVC	2	176
6	PCB	PVC	1.5	185
7	PCB	PVC	3	191

8	Optic	Germanium	4	205
9	Optic	Germanium	4	220
10	Optic	Germanium	4	245

3. RESULTS AND DISSCUSION

Numerical simulation of the interaction between the shaped charge jet and inhomogeneous obstacle was performed using the previously described setup and material models. Furthermore, additional simulation without the inhomogeneous obstacle was conducted with the aim to obtain insight into the differences in performances and properties of the formed jets. Those simulations have also provided information about the detonation wave propagation process, jet formation process and explosive reactive armor activation.

3.1. Detonation wave propagation

Detonation wave propagation in precursor shaped charge warhead is same for both of the analyzed cases as the obstacles don't have the influence on it. Sequence of plots depicting the evolution of the detonation wave may be seen in Fig.3. Observed warhead does not contain a wave shaper and thus, the detonation wave propagates in a spherical form. Detonation point was placed on the symmetry axis, in the rear end of explosive charge. Time needed for the completion of the detonation process was 6.617 μs. It is noteworthy to mention that the considered warhead is not designed optimally and that the jet and detonation properties could be enhanced.

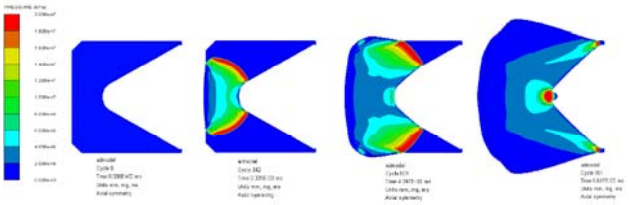

Figure 3. Detonation wave propagation in precursor shaped charge warhead

3.2. Jet formation process

Two simulation were performed: when the jet's path during the formation is unobstructed (Fig.4) and when the inhomogeneous obstacles are present (Fig.5).

In Fig.4 and Fig.5, sequences of jet formation process are displayed without the detonation products of the shaped charge's explosive and without the warhead's casing with the aim to provide better visualization of the jet.

Unobstructed jet had maintained approximately the same level of kinetic energy until it had achieved contact with the ERA's container when the minor drop of around 5% in its kinetic energy had occurred (Fig.6).

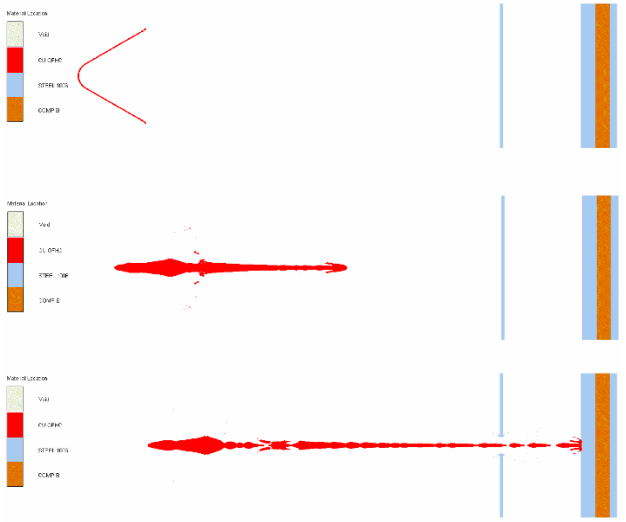

Figure 4. Jet formation process without obstacles

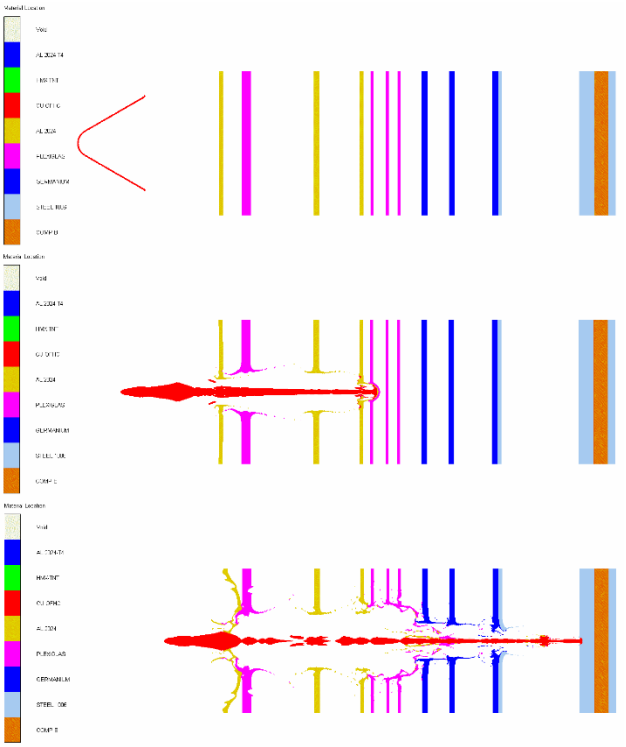

Figure 5. Jet formation process with inhomogeneous obstacle

In the case of the obstructed jet, jet formation process was characterized by several steep drops in the kinetic energy level and significant changes in the geometry of the primary jet due to the material bulking and localization that will lead to the jet particulation (Fig.5). Jet tip's encounter with each obstacle degrades the kinetic energy value in an approximately stepwise manner, as shown in Fig.6. It can also be noted that the time of the jet tip's impact into the ERA's front panel is not the same for both cases as there is a time delay in the obstructed case which is around 10 μs. This time period is highly important when the activation of the the main shaped charge warhead is considered, as it has to be done at a desired time and stand-off distance.

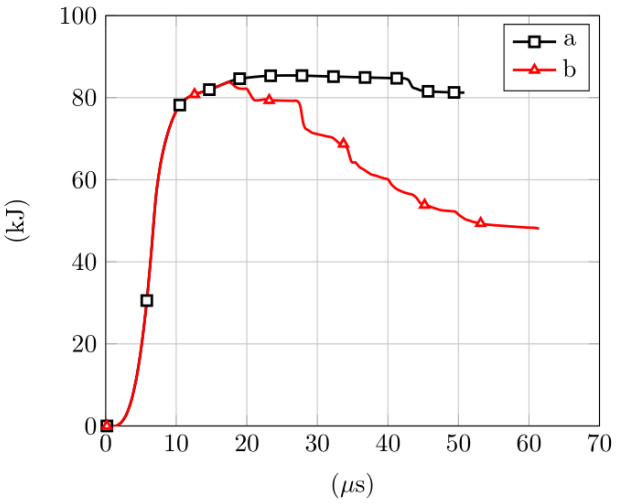

Figure 6. Cooper liner kinetic energy vs. time, a) without inhomogeneous obstacle, b) with inhomogeneous obstacle

By positioning the 29 fixed gauge points along the jet formation path, it was possible to observe jet's dynamic characteristics. Figure 7 shows the change in the jet tip velocity over time for both of the observed cases.

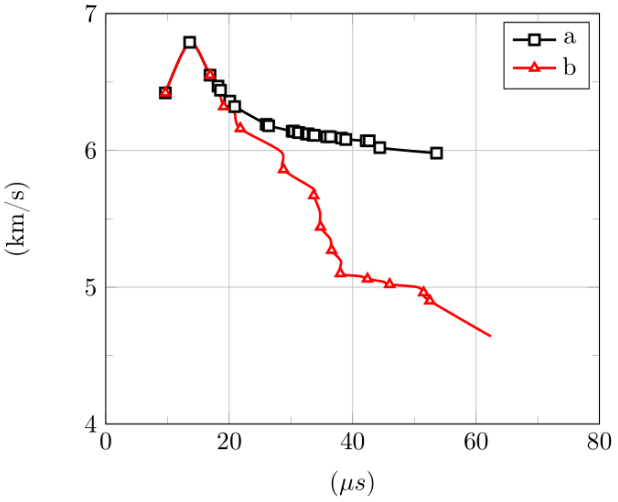

Figure 7. Jet tip velocity vs. time before impact into the ERA's front panel, a) without inhomogeneous obstacle, b) with inhomogeneous obstacle

In the case of the unobstructed jet formation, the jet tip velocity slightly decreases. Value of the jet tip velocity at the moment of its encounter with the ERA's front panel is 6km/s. On the other hand, in the case when the jet is obstructed by the inhomogeneous obstacles, jet tip's velocity drops significantly over time and forms a stepped profile that may be seen in Fig.7(b). In the moment of its impact into the ERA's front plate, velocity has the value of 4.6 km/s indicating the decrease of almost 25%.

Velocity gradient over the jet length is displayed in Fig.8 for both of the analyzed cases. For the unobstructed jet, its tip diameter is 5 mm and the maximum slug diameter is 10 mm. Total length of the jet in the moment of impact is 238.4 mm. For the case of the obstructed jet maximum jet tip diameter is 2.6 mm and maximum jet slug diameter is 11 mm, while the total length of the jet is 230 mm. As it may be seen, jet tip's diameter was reduced in size for almost 50%. On the other hand, change in the value of the jet's length is minor. According to the theoretical and the empirical criteria [9-12,14], formed jet meets the initiation conditions, even though it was heavily influenced by the inhomogeneous obstacles that have reduced its dynamic properties.

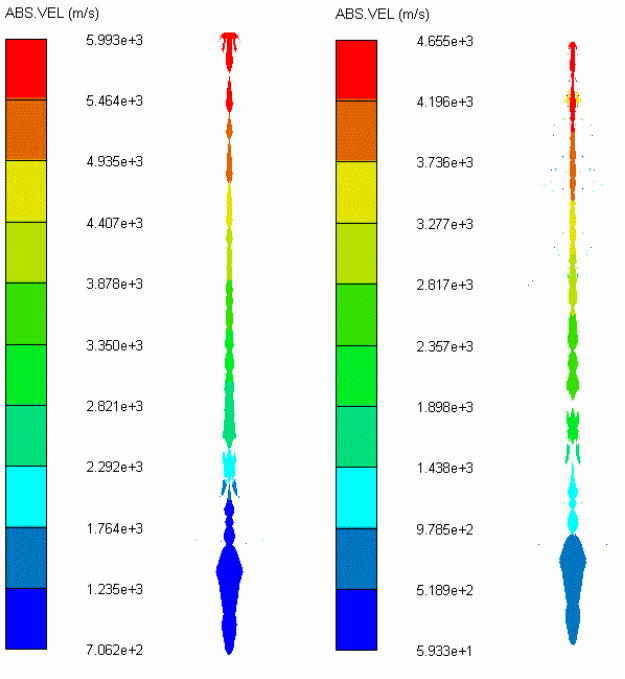

Figure 8. Velocity gradient in the jet at the moment of impact into the ERA'S front panel for the unobstructed (left figure) and obstructed (right figure) formation

3.2. Interaction of the jet and ERA

Upon the jet tip's impact into the ERA's front metal panel, large value of pressure was achieved in its material with the maximum of $3.086 \cdot 10^7$ kPa that was propagating towards the explosive. If the value of the shock wave pressure is smaller than Comp B's pre-bulk modulus, sufficient initiation energy won't be achieved. However, in the observed case the obstructed jet was able to induce the pressure of $5.2781 \cdot 10^6$ kPa in the Comp B which is enough to initiate explosive and create a hot spot at 65 μs, before the jet's tip had reached the front edge of the explosive. Figure 9 shows response of the ERA's explosive to the influence of the obstructed jet throughout the processes of its ignition and detonation wave propagation.

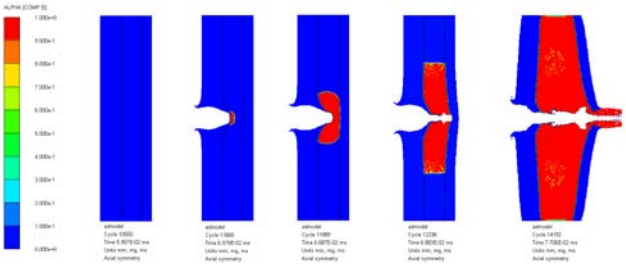

Figure 9. Sequences of ERA activation and change of the ALPHA coefficient

As an indicator of the explosive's current state, the reaction degree APLPHA was observed. In a case of a

complete explosive reaction its value is ALPHA=1, while for the unreacted explosive it is equal to zero (ALPHA=0). Part of the explosive that has not yet reached state of complete detonation is located between those two values (ALPHA=0-1). From Fig.9, conclusion can be made that after the jet penetrates through the first steel plate and initiates the explosive in 65 μs, the explosive continues to decompose and generates sufficient amount of energy which will lead to the initiation and growth of the explosive material in the radial direction. This is especially visible in the plots corresponding to the 66.87 μs and 68.83 μs. Complete detonation of the Comp B appears at 77.06 μs where the transfer of the energy from the detonation products onto the steel plates is clearly visible through their acceleration and displacement.

4. CONCLUSIONS

Following conclusions may be derived from the conducted study and thus obtained results:

- Numerical analysis of the jet formation process indicates that the inhomogeneous obstacles decrease the jet performance by the deterioration of the velocity gradient over its length. This is clearly evident when the jet tip velocity is being considered as its value had decreased for around 23% when compared to the unobstructed jet formation process. Furthermore, size of the jet tip diameter has been reduced for almost 50%.
- Even after the jet had penetrated through all of the inhomogeneous obstacles, he had enough energy to initiate ERA's explosive.
- Instead of the complex Lee-Tarver ignition and growth model for which the material parameters are hard to find in the open literature, simulations were performed by the implementation of the burn on compression coefficient and pre-bulk modulus. Calibration of these two coefficients should be made through the comparison of the simulation results with the experimentally obtained results.
- Analyzing explosive reactive armor activation time is important information for the main shaped charge warhead initiation. Numerical simulation can provide complete interaction analyses of precursor-shaped charge, main shaped charge warhead and explosive reactive armor.
- For future work it is recommended to analyze different angle position between missile and explosive reactive armor to determine threshold detonation angle. For maximum performances of precursor shaped charge warhead it must be analyzed with embedded wave shaper. Finally, the experimental validation of the obtained results is also planned.

ACKNOWLEDGEMENT

This research has been supported by the Ministry of Education, Science and Technological Development of the Republic of Serbia, through the subproject III-47029, in the 2022 year, which is gratefully acknowledged.

References

[1] Орленко,Л.П. : Физика Взрыва, Главная редакция физико-математической литературы, Москва, (2004).

[2] CORLEONE,J.: Tactical Missile Warheads, American Institute of Aeronautic and Astronautic, Washington, (1993).

[3] UGRČIĆ,M. et al.: *Characterization of the natural fragmentation of explosive ordnance using the numerical techniques based on the FEM*, Scientific Technical Review, 65, (2015), 16-27.

[4] UGRČIĆ,M. et al.: *Fem techniques in shaped charge simulation*, Scientific Technical Review, 59, (2009), 26-34.

[5] MARKOVIĆ,M. et al.: *Numerical and analytical approach to the modeling of explosively formed projectiles*, 6th international scientific conference on defensive technologies, (2014), 1-7.

[6] MARKOVIĆ,M. et al.: *Comparative approaches to the modeling of explosively formed projectiles*, Proceedings of Tomsk State University, 293, (2014).

[7] MARKOVIĆ,M. et al.: *Simulation of changes in temperature and pressure fields during high speed projectiles forming by explosion*, Thermal science, 20, (2016), 1714-1752.

[8] JEREMIĆ,O., et al.: *Analytical and numerical method of velocity fields for the explosively formed projectiles*, FME Transactions, 45, (2017), 38-44.

[9] YANAN,DU. et al.: *Study on penetration performances of rear shaped charge warhead*, Materials, 14, (2021), 1-17.

[10] CHANG,B.H. et al.: *Numerical simulation of modified low-density jet penetrating shell charge*, International journal of simulation model, 14, (2015), 426-437.

[11] LIANGLIANG,D., et al.: Simulation study on jet formability and damage characteristics of a low-density material liner, Materials, 11, (2018), 1-17.

[12] UGRČIĆ,M.: Prilog teoriji interakcije eksplozivnog oklopa I kumulativnog projektila, Doktorska disertacija, (1995).

[13] PAPPU,S., MURR,L.E.: Hydrocode and microstructural analysis of explosively formed penetrators, Journal of Materials Science, (2002), 233-248.

[14] UGRČIĆ,M., et al.: *Teorijski aspekti I numerička simulacija kumulativnog efekta*, Kumulativna naučnotehnička informacija, Vojnotehnički institut – Beograd, (2012).